JOURNAL OF SOLID STATE CHEMISTRY **127,** 9–18 (1996)
ARTICLE NO. 0350

Structure, Thermal Behavior and IR Investigation of a New Organic Cyclohexaphosphate

Miriem Charfi and Amor Jouini[1]

Laboratoire de Chimie du Solide, Département de Chimie Faculté des Sciences, Université du Centre, Monastir, 5000, Tunisia

Received April 17, 1996; in revised form July 18, 1996; accepted July 24, 1996

Physicochemical properties of the bis[1-(2-ammoniumethyl) piperazinium] cyclohexaphosphate hexahydrate are discussed on the basis of X-ray crystal structure investigation. $[C_6H_{18}N_3]_2P_6O_{18}\cdot 6H_2O$ is triclinic, $P\bar{1}$, with $a = 9.714(2)$ Å, $b = 10.538(2)$ Å, $c = 8.095$ Å, $\alpha = 87.88(2)°$, $\beta = 93.48(2)°$, $\gamma = 83.20(1)°$, and $Z = 1$. The structure has been solved using direct methods and refined to a reliability R factor of 0.0307 for 2291 reflections. The compound is characterized by infinite layers of inorganic polyanions approximately parallel to the (0 0 1) planes. Organic cations are sandwiched between these layers. OW–H $\cdots$ O and N–H $\cdots$ O hydrogen bonds link P_6O_{18} groups, respectively, in a layer and in successive layers as to build a framework in a three-dimensional way. Two water molecules leave this compound at room temperature giving a stable tetrahydrate phase. The structure reorganization is discussed on the basis of OW H-bonds by TG-DTA and DSC thermal analyses. The reported IR study is supported by a detailed theoretical group analysis applied to P_6O_{18} with D_{6h} ideal local symmetry.

I. INTRODUCTION

The recent crystal chemistry investigation of compounds resulting from encapsulation of organic molecules between chains or layers of cyclohexaphosphate anions does not provide a sufficient number of representatives for comparison of their basic chemical properties with those of other compounds such as cyclotriphosphates or cyclotetraphosphates. The lack of a good starting material and of a reliable process producing single crystals of organic cyclohexaphosphates are probably the main reasons for the poorness of this class of organic condensed phosphates. Ever since the process for preparing $Li_6P_6O_{18}$ (1) as starting material has been known, the use of ion-exchange resins became valuable for the production of organic cyclohexaphosphates. The two cyclohexaphosphates with linear organic molecules $[C_4H_{16}N_3]_2P_6O_{18}\cdot 2H_2O$ (2) and $[C_6H_{18}N_2]_3P_6O_{18}\cdot 6H_2O$ (3) were obtained by this way. The present work deals with crystal structure determination and physicochemical properties of a new organic cyclohexaphosphate prepared with the same interaction route. The linear organic molecule is replaced by a polarizable cyclic organic cation inducing an isotropic crystal growth which reflects the role played by the strong three-dimensional hydrogen-bond network.

[1] To whom correspondence should be addressed.

II. CRYSTAL CHEMISTRY

II.1. Chemical Preparation

Most of the well characterized organic cyclohexaphosphates were prepared in two steps: (i) a dilute solution of cyclohexaphosphophosphoric acid (0.035 *M*/liter) was prepared from 12 g of $Li_6P_6O_{18}$ using ion-exchange resins (Amberlite IR 120), and (ii) the acid produced is immediately neutralized by the stoichiometric amount of 1-(2-aminoethyl) piperazin (6 cm^3, density 0.981). Schematically the reaction is

$$2\,C_6H_{15}N_3 + H_6P_6O_{18} \xrightarrow{(H2O)} [C_6H_{18}N_3]_2P_6O_{18}\cdot 6H_2O.$$

The resulting solution, slowly evaporated at room temperature for several weeks, leads to transparent, thin single crystals not very stable under normal conditions of temperature and humidity. Indeed, the title compound is converted to a tertrahydrate phase over a six month period under normal conditions.

II.2. Crystal Data and Structure Determination

The unit-cell dimensions have been measured and refined using a set of 25 high-angle reflections collected with an Enraf-Nonius CAD4 diffractometer. The average density, measured at room temperature using toluene as pycnometric liquid, is in agreement with the calculated density. The cell contains one formula unit of the title compound. The parameters used for X-ray data collection, crystal structure determination, and final results are reported in Table 1. The final atomic coordinates and the U equivalent

0022-4596/96 $18.00

TABLE 1
Main Crystallographic Features, X-Ray Diffraction Data Collection Parameters of $[C_6H_{18}N_3]_2P_6O_{18} \cdot 6H_2O$, and Its Finals Results

I. Crystal data	
Formula: $(C_6H_{19}N_3)_2P_6O_{18} \cdot 6H_2O$	$Fw = 846.38$
Crystal system: triclinic	Space group: $P\bar{1}$
$a = 9.7149(2)$, $b = 10.538(2)$	$V = 820.5(3)$ Å^3
$c = 8.095(2)$ Å, $\alpha = 87.88(2)°$	
$\beta = 93.48(2)°$, $\gamma = 83.20(1)°$	$Z = 1$
$\rho_{cal.}$, $\rho_{mes.} = 1.71$, 1.64 g cm^{-3}	$F(000) = 444$
Linear absorption factor:	$\mu(\text{Ag}K\alpha) = 0.430$ mm^{-1}
Morphology:	elongated prism
Crystal size:	$0.17 \times 0.20 \times 0.28$ mm
II. Intensity measurements	
Temperature: 293 K	Wavelength: Mo$K\alpha$(0.71069 Å)
Diffractometer: Nonius CAD4	Scan mode: $\omega/2\theta$
Monochromator: graphite plate	Scan width: 1.20°
Variable scan speed	$T_{max.}$ per scan: 60 s
Theta range:	3°–25°
Background measuring time:	$T_{max.}/2$
Measurement area: $\pm h$, $\pm k$, l	$h_{max.} = 11$, $k_{max.} = 12$, $l_{max.} = 9$
Number of scanned reflections:	3109
Number of unique reflections:	2888 ($R_{int.} = 0.012$)
One reference reflection:	every 2 hr, intensity
decay: 0.58%	
III. Structure determination	
Lorentz and polarization corrections	No absorption correction
Structure determination:	Direct Methods: SHELXS86 (4)
Structure refinement with	SHELXL93 (5) on PC Computer
Unique reflections included:	2291 with $I > 2\sigma(I)$
Refined parameters: 314	Atomic scattering factors from International Tables for Crystallography (1992, Vol. C, Tables 4, 2, 6, 8 and 6, 1, 1, 4)
All H atom parameters refined	
Refinement on F	
$S = 1.122$	
Secondary extinction coefficient:	0.0084 (24)
Unweighted R factor = 0.0307	weighted R factor $WR = 0.1140$
$W = 1/[\sigma^2(F_o^2) + (0.0317P)^2 + 1.2088P]$	$P = (F_o^2 + 2F_c^2)/3$
$\Delta\rho_{max} = 0.393$ e Å^{-3}	Largest shift/error = 0.001

temperature factors (isotropic for H atoms) are given in Table 2. The values of the thermal anisotropic displacement parameters for nonhydrogen atoms and the list of observed and calculated structure factors are available upon request to the authors.

II.3. Thermal Behavior

Setaram thermoanalyzers, TG-DTA92 and DSC92, are used to perform thermal treatment on samples of the title compound. The TG-DTA experiments are made with 27.5 mg samples in an open alumina crucible. The DSC analysis is carried out using weighted 10 mg samples sealed in an aluminum DSC crucible. In both techniques, samples are heated in air with a 5 K/min heating rate, from 300 to 625 K; an empty crucible is used as reference.

II.4. Infrared Spectroscopic Investigation

Infrared spectra were recorded using a Perkin-Elmer 983 spectrometer. Samples were dispersed in KBr and scanning was performed in the 4000–200 cm^{-1} spectral domain with a resolution of about 3 cm^{-1}.

III. STRUCTURE DESCRIPTION

The atomic arrangement can be described by layers of the inorganic entities approximately parallel to the (**a**, **b**) planes. Cohesion between these planes is established by H bonds from the organic entities. Figure 1 gives a projection, along the **b** direction, of this atomic arrangement. Adjacent P_6O_{18} groups are linked pairwise with OW1 water molecules so as to form an infinite chain spreading along the **a**

TABLE 2
Final Atomic Coordinates and U_{eq} (U_{iso} for H atoms) of $[C_6H_{18}N_3]_2P_6O_{18} \cdot 6H_2O$

Atoms	$x(\sigma)$	$y(\sigma)$	$z(\sigma)$	$U_{eq.}$ (Å^2)
P1	0.6578(1)	0.7872(1)	0.0979(1)	0.0202(2)
P2	0.7684(1)	0.0281(1)	0.1412(1)	0.0202(2)
P3	0.4544(1)	0.7648(1)	−0.1831(1)	0.0206(2)
OE11	0.6371(2)	0.7819(2)	0.2771(3)	0.0281(5)
OE12	0.7610(2)	0.6917(2)	0.0277(3)	0.0285(5)
OL12	0.6929(2)	0.9270(2)	0.0379(3)	0.0272(5)
OL13	0.5085(2)	0.7866(2)	0.0051(3)	0.0299(6)
OE21	0.8232(2)	0.1145(2)	0.0185(3)	0.0277(5)
OE22	0.8638(2)	0.9631(2)	0.2751(3)	0.0284(5)
OL23	0.6408(2)	0.1020(2)	0.2283(3)	0.0270(5)
OE31	0.3684(3)	0.6593(2)	−0.1749(3)	0.0351(6)
OE32	0.5696(2)	0.7579(2)	−0.2949(3)	0.0313(6)
OW1	0.9423(3)	0.7951(3)	−0.1742(4)	0.0370(6)
OW2	0.1255(4)	0.6116(3)	−0.3153(4)	0.0509(8)
OW3	0.8119(3)	0.6075(3)	0.4792(4)	0.0458(7)
N1	0.7583(3)	0.5111(2)	−0.2161(4)	0.0283(6)
N2	0.7825(3)	0.2399(2)	−0.2775(3)	0.0196(6)
N3	0.7473(3)	0.9109(3)	−0.4228(4)	0.0272(6)
C1	0.8836(4)	0.4235(3)	−0.1571(5)	0.0310(8)
C2	0.9069(3)	0.3127(3)	−0.2676(4)	0.0257(7)
C3	0.6575(4)	0.3287(3)	−0.3396(5)	0.0283(7)
C4	0.6336(4)	0.4410(4)	−0.2273(5)	0.0343(8)
C5	0.8095(3)	0.1271(4)	−0.3809(4)	0.0241(7)
C6	0.6949(4)	0.0406(4)	−0.3714(4)	0.0245(7)
H1W1	0.901(5)	0.773(5)	−0.103(6)	0.06(2)*
H2W1	0.011(6)	0.841(5)	−0.129(7)	0.08(2)*
H1W2	0.200(5)	0.627(4)	−0.266(5)	0.04(1)*
H2W2	0.064(7)	0.675(6)	−0.268(8)	0.11(2)*
H1W3	0.836(4)	0.548(4)	0.420(5)	0.03(1)*
H2W3	0.755(5)	0.661(5)	0.413(6)	0.05(1)*
H1N1	0.743(4)	0.575(4)	−0.151(5)	0.04(1)*
H2N1	0.772(4)	0.549(4)	−0.322(4)	0.04(1)*
HN2	0.777(3)	0.213(3)	−0.178(5)	0.02(9)*
H1N3	0.676(3)	0.861(3)	−0.402(4)	0.01(7)*
H2N3	0.8824(5)	0.881(4)	−0.353(6)	0.04(1)*
H3N3	0.770(4)	0.914(4)	−0.520(6)	0.04(1)*
H1C1	0.860(4)	0.396(4)	−0.047(5)	0.03(1)*
H2C1	0.963(4)	0.472(4)	−0.163(5)	0.03(1)*
H1C2	0.985(4)	0.251(3)	−0.224(4)	0.03(1)*
H2C2	0.923(4)	0.344(3)	−0.381(5)	0.03(1)*
H1C3	0.579(4)	0.291(3)	−0.333(4)	0.02(1)*
H2C3	0.670(4)	0.359(4)	−0.453(5)	0.03(1)*
H1C4	0.551(4)	0.500(4)	−0.274(5)	0.04(1)*
H2C4	0.620(5)	0.410(4)	−0.120(6)	0.05(1)*
H1C5	0.894(4)	0.083(4)	−0.344(5)	0.02(1)*
H2C5	0.814(4)	0.153(4)	−0.485(6)	0.04(1)*
H1C6	0.667(3)	0.033(3)	−0.275(4)	0.01(1)*
H2C6	0.609(4)	0.075(4)	−0.439(5)	0.04(1)*

Note. Starred atoms were refined isotropically. e.s.d.s are given in parentheses. $U_{eq.} = 1/3\Sigma_i\Sigma_j U_{ij}a_i^*a_j^*a_ia_j$.

direction. The remaining OW2 and OW3 link infinite chains to give rise to infinite layers centered approximately by the (0 0 1) planes and depicted in Fig. 2. In fact, the water molecules of this layer are not, as it is most frequently observed, dispersed inside the atomic arrangement. They are assembled in groups of six, building an irregular hexagon 2[OW2 $\cdots$ OW1 $\cdots$ OW3], located around the (0, 1/2, 1/2) inversion center of the unit cell and with the following edge lengths: OW1 $\cdots$ OW2 = 2.794(4) Å, OW1 $\cdots$ OW3 = 3.736(4) Å, and OW2 $\cdots$ OW3 = 2.730(5) Å. The average OW $\cdots$ OW $\cdots$ OW angle, in this hexagonal cluster, is 118.3(5)°. It is worth noting that among the 12 H atoms belonging to the water molecules inside this hexagon, only 4 establish hydrogen bonds between OW1, OW2, and OW3. The remaining ones are involved in H bonds with external oxygen atoms of the P_6O_{18} groups as to build the layer described above. Similar polygonal clusters of water molecules have been observed in other condensed phosphates: an almost regular pentagon in $Li_4P_4O_{12} \cdot 5H_2O$ (6), hexagons of symmetry $\bar{1}$ in $Ni(NH_4)_2\ P_4O_{12} \cdot 7H_2O$ (7) and of symmetry $\bar{3}$ in $Cd_3P_6O_{18} \cdot 6H_2O$ (8). The centrosymmetric ring anion $P_6O_{18}^{6-}$ is located around the inversion center at (1/2, 0, 0) and so is built up by only three independent PO_4 tetrahedra.

III.1. The P_6O_{18} Geometry

Despite the small number of representatives, the examination of the main geometric features of the P_6O_{18} rings seems worthwhile. The P–P distances and P–O–P angles are similar to what is commonly observed in other condensed phosphoric anions, mainly in P_3O_9 and P_4O_{12}. The average of the P–P distances is 2.927(1) Å and the range of the observed values is narrow, the extreme values being 2.896(1) and 2.956(1) Å. The P–O–P angles, in this group, have typical values of condensed phosphoric anions, with an average value of 131.8(1)° and extrema of 128.8(1)° and 134.3(2)°. Meanwhile, if we compare the observed P–P–P angles in the P_6O_{18} group with those in well-represented types of phosphoric rings, such as P_3O_9 and P_4O_{12}, we observe a very large deviation from the ideal value, 120°. In P_3O_9 and P_4O_{12} groups, the P–P–P angles never depart significantly from their ideal values, 60 ± 2° for P_3O_9 (9) and 90 ± 4° for P_4O_{12} (9). In contrast, these P–P–P angles in the case of P_6O_{18} ring anion exhibit very large deviations from the 120° ideal value, the average angle being 111.33(4)° with extrema of 103.99(4)° and 119.14°. It is to be noted that there is a rather regular distribution of the P–P–P angles, in this compound, with 5.15° between extrema values. The largest difference between extrema, observed in the P_6O_{18} anion with $\bar{1}$ internal symmetry, like in the title compound is of 50° (10), where the lowest one, close to zero, is found in the P_6O_{18} group with high symmetry $\bar{3}$ (11), and built by one PO_4 tetrahedron. Thus the lowest strain allows this group to adopt more configurations than the P_3O_9 and the P_4O_{12} groups. The main geometrical features of P_6O_{18} group are reported in Table 3.

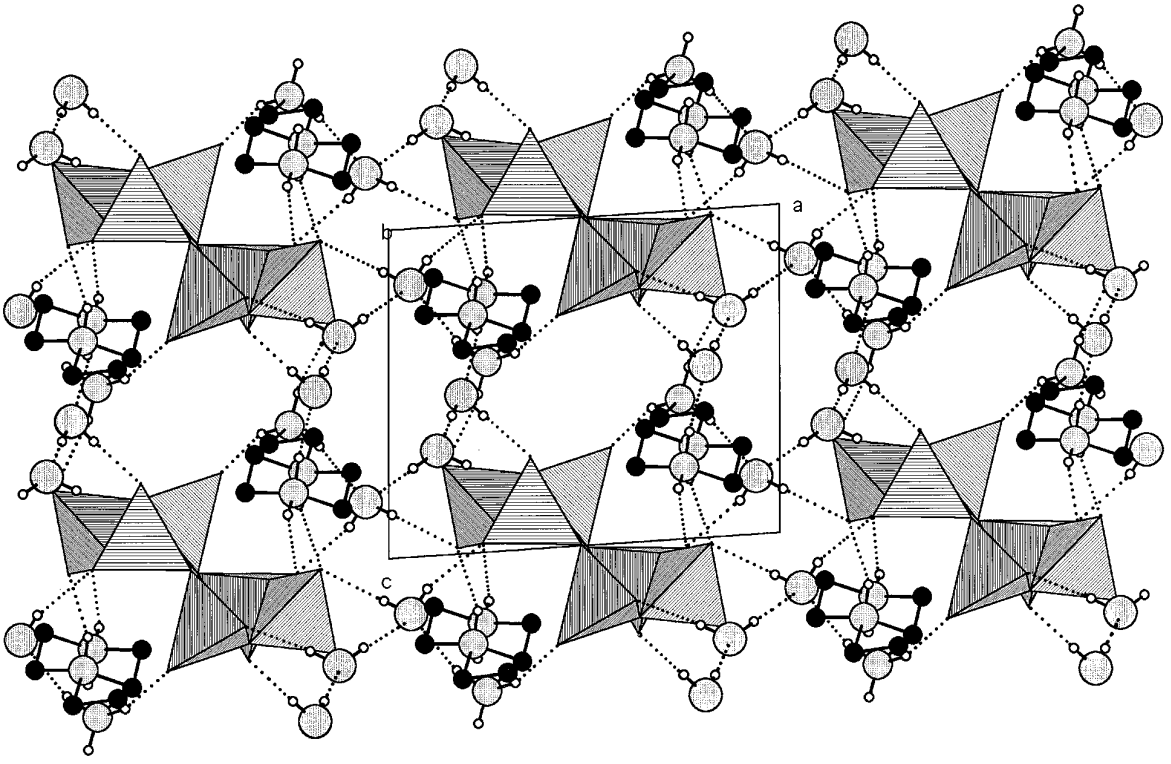

FIG. 1. Projection along the **b** direction of the atomic arrangement. P_6O_{18} groups are given with a polyhedral representation. By order of decreasing sizes, circles represent oxygen water molecules and nitrogen atoms. The black and white smaller circles indicate carbon and hydrogen atoms. Hydrogen bonds are denoted by full and dotted lines.

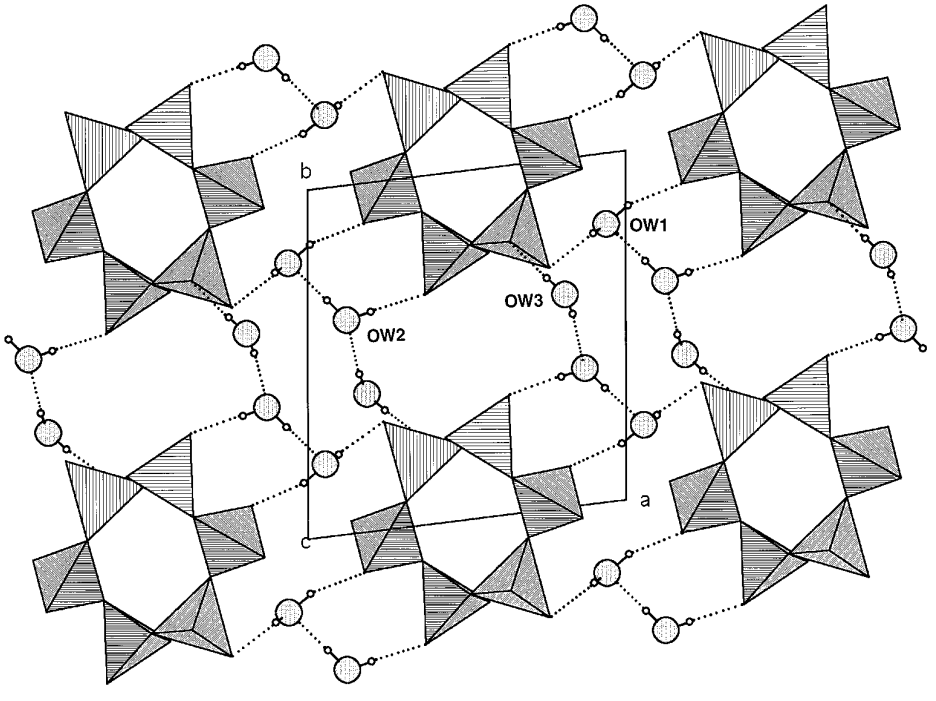

FIG. 2. Projection along the **c** direction of the anionic layer with P_6O_{18} groups in polyhedral representation and oxygen water molecules with large circles. Hydrogen bonds are denoted by full and dotted lines.

TABLE 3
Main Interatomic Distances (Å) and Bond Angles (°) in the P_6O_{18} Group

		$P(1)O_4$ tetrahedron		
P1	OE11	OE12	OL12	OL13
OE11	1.477(2)	120.1(1)	110.8(1)	106.5(1)
OE12	2.568(3)	1.478(2)	107.0(1)	110.4(1)
OL12	2.547(3)	2.495(3)	1.615(2)	100.3(1)
OL13	2.461(3)	2.530(3)	2.463(3)	1.593(2)
		$P(2)O_4$ tetrahedron		
P2	OE21	OE22	OL12	OL23
OE21	1.487(2)	119.1(1)	106.7(1)	110.6(1)
OE22	2.554(3)	1.475(2)	110.9(1)	106.6(1)
OL12	2.475(3)	2.531(3)	1.597(2)	101.4(1)
OL23	2.539(3)	2.468(3)	2.474(3)	1.600(2)
		$P(3)O_4$ tetrahedron		
P3	OE31	OE32	OL13	OL23
OE31	1.469(2)	119.4(1)	106.5(1)	110.5(1)
OE32	2.546(3)	1.478(2)	111.4(1)	106.8(1)
OL13	2.472(3)	2.556(3)	1.615(2)	100.8(1)
OL23	2.526(3)	2.475(3)	2.480(3)	1.604(2)

P1–P2 2.896(1) P2–P1–P3 119.14(4)
P1–P3 2.931(1) P1–P2–P3 111.03(4)
P2–P3 2.956(1) P1–P3–P2 103.99(4)

P1–OL12–P2 128.8(1)
P1–OL13–P3 134.3(1)
P2–OL23–P3 132.3(1)

Note. e.s.d.s are given in parentheses.

III.2. The Organic Group

Organic cations are sandwiched between (0 0 1) planes. The anionic layers parallel to the (**a**, **b**) plane are stabilized by the hydrogen bond network. Each organic trication is anchored onto successive layers through N–H···O bonds. Taking into account the main work on structural evidence of C–H···O bonds in molecular crystals (12–15), the C–H···O interactions contribute, to a lesser degree than O–H···O and N–H···O, to the cohesion of the structure. Thus, three types of hydrogen bonds occur in this atomic arrangement: (i) OW–H···O, including 6 relatively short contacts with H···O distances ranging from 1.83(5) to 2.01(6) Å, ensure the cohesion between anions in the layer; (ii) N–H···O involving 6 short contacts with H···O distances, in the range 1.77(5)–2.02(5) Å, link parallel layers; (iii) C–H···O bonds are formed by 12 relatively weak contacts, since the H···O(N) distances, ranging from 2.37(4) to 2.93(4) Å. The third type of hydrogen bond, linking successive anionic layers, increases the structural cohesion. The mean value of the C–H···O angle 145.9° is smaller than the mean O(N)–H···O hydrogen bond angle 167.2°. This may be ascribed to the fact that the O(N)–H···O hydrogen bonds are shorter than the C–H···O contacts. Consequently, the O(N)···O van der Waals repulsion is likely to be larger than the C···O repulsion for a given value of the O(N, C)–H···O angle. The O(N)···O distance, frequently designed in the literature as hydrogen bond criteria, is of lesser interest, thus, in the geometric characterization of hydrogen bond, the focus must be rather pointed on the H···O distance and on the O(N, C)–H···O angle than the O(N)···O distance, It is to be noted that the C6 involves its H atoms with two oxygen atoms (OL) linking phosphores in the P_6O_{18} ring. This fact is rarely observed in so far as OL atoms are uncommonly found in metallic cation polyhedra coordinations of inorganic phosphates. The main geometric features of the organic groups and of the hydrogen bonds are assigned in Tables 4 and 5.

III.3. The Water Molecule Coordination

It is well known that the preferred hydrogen bond coordination of the water molecules is tetrahedral or planar trigonal. However many different configurations, with lower or higher coordination, are observed in solid state chemistry. Taking into account the C–H–OW interactions,

TABLE 4
Main Interatomic Distances (Å) and Bond Angles (°) in the Organic Group

N1–H1N1 0.88(4)			
N1–H2N1 0.95(4)		H1N1–N1–H2N1 106(4)	
N2–HN2 0.85(4)			
N3–H1N3 0.94(3)		H1N3–N3–H2N3 109(3)	
N3–H2N3 0.93(5)		H1N3–N3–H3N3 116(3)	
N3–H3N3 0.83(5)		H2N3–N3–H3N3 110(4)	
C1–H1C1 0.98(4)			
C1–H2C1 0.98(4)		H1C1–C1–H2Cl 117(3)	
C2–H1C2 0.98(4)			
C2–H2C2 0.99(4)		H1C2–C2–H2C2 106(2)	
C3–H1C3 0.91(4)			
C3–H2C3 0.98(4)		H1C3–C3–H2C3 112(3)	
C4–H1C4 1.00(4)			
C4–H2C4 0.94(5)		H1C4–C4–H2C4 111(4)	
C5–H1C5 0.93(3)			
C5–H2C5 0.88(4)		H1C3–C3–H2C3 109(3)	
C6–H1C6 0.85(4)			
C6–H2C6 0.99(4)		H1C4–C4–H2C4 103(3)	
N1–C1	1.481(5)	N1–C1–C2	111.2(3)
C1–C2	1.501(5)	C1–C2–N2	110.9(3)
C2–N2	1.506(4)	C2–N2–C3	109.1(3)
N2–C3	1.491(4)	N2–C3–C4	110.8(3)
C3–C4	1.523(5)	C3–C4–N1	110.3(3)
C4–N1	1.492(5)	C4–N1–C1	110.6(3)
N2–C5	1.486(4)	C2–N2–C5	110.3(2)
C5–C6	1.524(5)	C3–N2–C5	113.1(3)
C6–N3	1.485(4)	N2–C5–C6	111.3(3)
		C5–C6–N3	109.4(3)

Note. e.s.d.s are given in parentheses.

TABLE 5
Bond Lengths (Å) and Angles (°) in the Hydrogen-Bonding Scheme

	N(O, C)–H	H···O	N(O, C)···O	N(O, C)–H···O
N1–H1N1···OE12	0.89(4)	1.95(4)	2.794(4)	162(4)
N1–H2N1···OW3	0.95(4)	1.79(4)	2.735(4)	174(4)
N2–HN2···OE21	0.85(4)	1.87(4)	2.678(3)	159(3)
N3–H1N3···OE32	0.94(3)	1.82(3)	2.721(4)	161(3)
N3–H2N3···OW1	0.93(5)	1.92(5)	2.817(4)	163(4)
N3–H3N3···OE22	0.83(5)	2.02(5)	2.819(4)	162(4)
OW1–H1W1···OE12	0.78(6)	2.01(6)	2.763(4)	163(5)
OW1–H2W1···OE21	0.92(6)	1.92(6)	2.818(4)	163(5)
OW2–H1W2···OE31	0.84(5)	1.83(5)	2.667(4)	176(4)
OW2–H2W2···OW1	0.95(7)	1.84(7)	2.794(4)	179(6)
OW3–H1W3···OW2	0.82(4)	1.92(4)	2.730(5)	168(4)
OW3–H2W3···OE11	0.88(5)	1.88(5)	2.764(4)	178(4)
C1–H1C1···OW2	0.98(4)	2.93(4)	3.836(5)	155(3)
C1–H2C1···OW2	0.98(4)	2.61(4)	3.517(5)	154(3)
C2–H1C2···OE22	0.98(4)	2.60(4)	3.451(4)	145(3)
C2–H2C2···OW3	0.99(4)	2.84(4)	3.479(5)	123(3)
C3–H1C3···OE11	0.91(4)	2.38(4)	3.275(4)	169(3)
C3–H2C3···OW2	0.98(4)	2.85(4)	3.680(5)	143(3)
C4–H1C4···OE31	1.00(4)	2.49(4)	3.303(5)	138(3)
C4–H2C4···OE31	0.94(5)	2.46(5)	3.388(3)	168(4)
C5–H1C5···OE22	0.93(4)	2.37(4)	3.256(4)	160(3)
C5–H2C5···OE22	0.88(4)	2.86(4)	3.367(4)	118(3)
C6–H1C6···OL12	0.85(4)	2.71(4)	3.483(4)	152(3)
C6–H2C6···OL23	0.99(4)	2.74(4)	3.279(4)	115(3)
H1W1–OW1–H2W1	108(5)	H1W2–OW2–H2W2		98(5)
	H1W3–OW3–H2W3	104(4)		

Note. e.s.d.s are given in parentheses.

four water molecules 2(OW1 + OW2) have a tetrahedral coordination, and the other two 2OW3 are rather in planar trigonal configuration and are less strongly bonded to the atomic arrangement. The water molecule OW1 (Fig. 3) accepts two short hydrogen bonds, one from the NH_3^+ cation, the other from OW2, to form an almost regular tetrahedron, whereas the OW2, in a rather distorted tetrahedron, accepts a short hydrogen bond from OW3 and a relatively short C1–H···OW2 interaction. Neglecting the very weak C2–H2···OW3 interaction, the coordination of OW3 would be regarded as roughly trigonal-planar, whereas it is actually in very distorted tetrahedral coordination. These observations suggest that CH donors are able to complete the tetrahedral hydrogen bond geometries of water molecules if a sufficient number of OH and NH is not available. However, it is to be noted that, in this case, the CH contact in the local environment of OW3 is weak since the corresponding distance H···O is 2.84 Å (cf. Fig. 3).

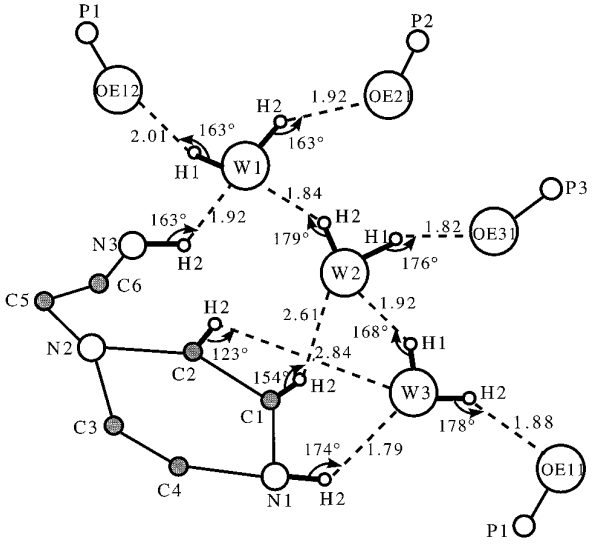

FIG. 3. Schematic H-bond scheme in the water molecule coordination.

IV. THERMAL BEHAVIOR

The TG-DTA thermograms depicted in Fig. 4 are obtained on a six-month-old specimen of the title compound. The removal of most of the water molecules, observed in the temperature range 339–423 K, is related to the first endothermic peak on the DTA curve with maximum elimination at 398 K. With further increase in temperature, the sample loses the remaining water and melts in one step with maximum temperature at 490 K. Indeed the TG curve

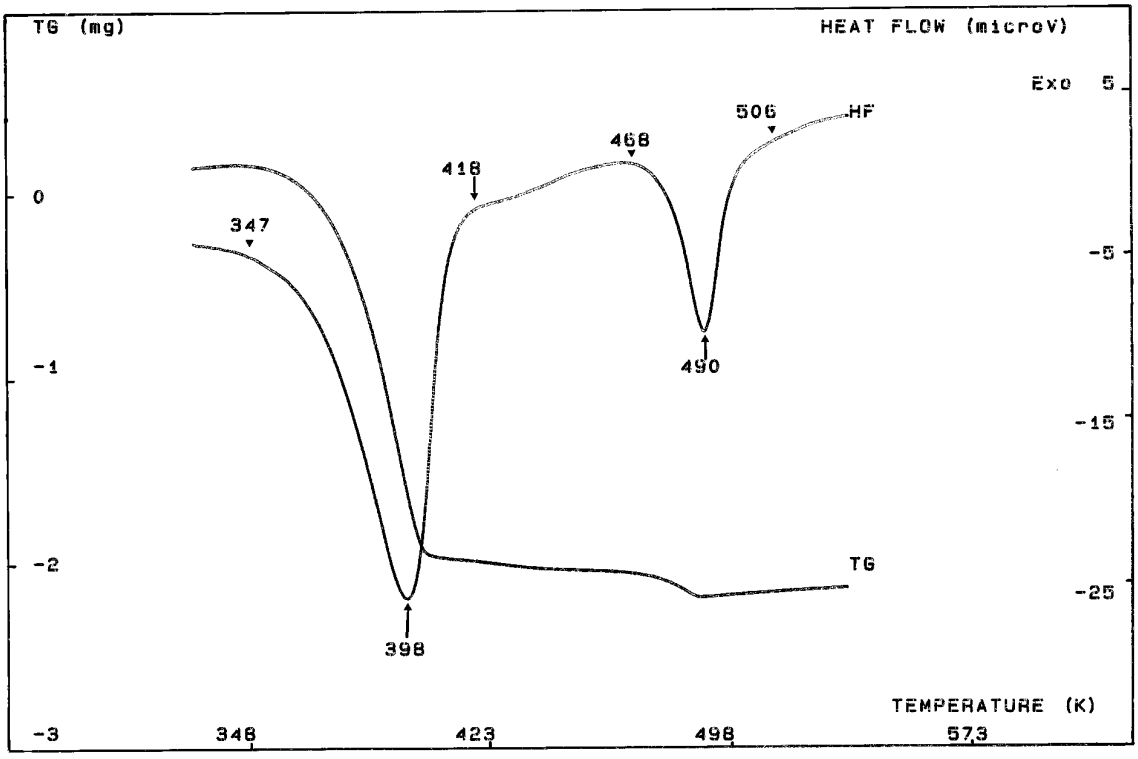

FIG. 4. TG-DTA analysis on the tetrahydrate phase resulting from the dehydration of $[C_6H_{18}N_3]_2P_6O_{18} \cdot 6H_2O$ under normal conditions.

shows, after the first H_2O elimination, a rather small and continuous weight loss (0.68%) from 421 K to the upper limit of the melting temperature. Thus, the second endothermic peak must be regarded, in fact, as a combination of the remaining H_2O elimination and melting of the anhydrous compound. This melting point, occurring without decomposition, is confirmed by an additional thermal treatment in a separate carbolite furnace with run heating of 5 K/min from room temperature to 493 K, the resulting compound being a white liquid. However, only four water molecules can be deduced from the TG curve. On the other hand, the DSC thermogram registered on ground fresh samples (Fig. 5a) exhibits also two endothermic effects. Nevertheless, the first shouldered one, corresponding to the dehydration, in the range from 380 to 410 K, shows the existence of more than one type of water molecule. The overall ΔH of the dehydration is 179.78 kJ/mol. The second endothermic peak occurring in the temperature range 475–504 K corresponds to the melting with a ΔH fusion of 26.649 kJ/mol. Furthermore, the DSC thermogram (Fig. 5b) recorded on a six-month-old sample reveals some interesting features, the most remarkable being that the left shoulder of the endothermic peak dehydration, mentioned to be at 386 K (Fig. 5a), is split into an inflection at 380 K and a symmetric intense peak at 390 K, whereas the intense endothermic peak at 405 K is strongly decreased. The derivative of the heat flow emphasizes clearly the water molecule reorganization at room temperature. Having in mind the number of water molecules located in the structure determination on a fresh crystal and on the basis of the thermal analysis, one can deduce that when the compound was left standing for an extended period of time under normal conditions it lost two water molecules. Thereafter, a structural rearrangement was performed involving the reorganization of hydrogen bonds in the sphere of coordination of the remaining water molecules. Thus, the thermal behavior confronted with the results of this crystal structure (cf. Section III.3), having crystallographic quality factor <0.031, can probably explain the departure of the two water molecules from the title compound under ambient conditions over a six month period.

V. IR INVESTIGATION

Infrared data on cyclohexaphosphates are very rare and only two articles dealing with this class have been reported. They described the IR spectra of P_6O_{18} ring anion with a mineral cation in $Cr_2P_6O_{18} \cdot 21H_2O$ (16) and with an organic cation in $[C_4H_{16}N_3]_2P_6O_{18} \cdot 2H_2O$ (2). It is worth noting that the IR spectrum in the above organic compound concerns an isolated P_6O_{18} ring in the cell whence the coupling between anions is avoided. Also, this spectrum is supported by a detailed theoretical group analysis applied to an isolated P_6O_{18} group in its ideal D_{6h} local sym-

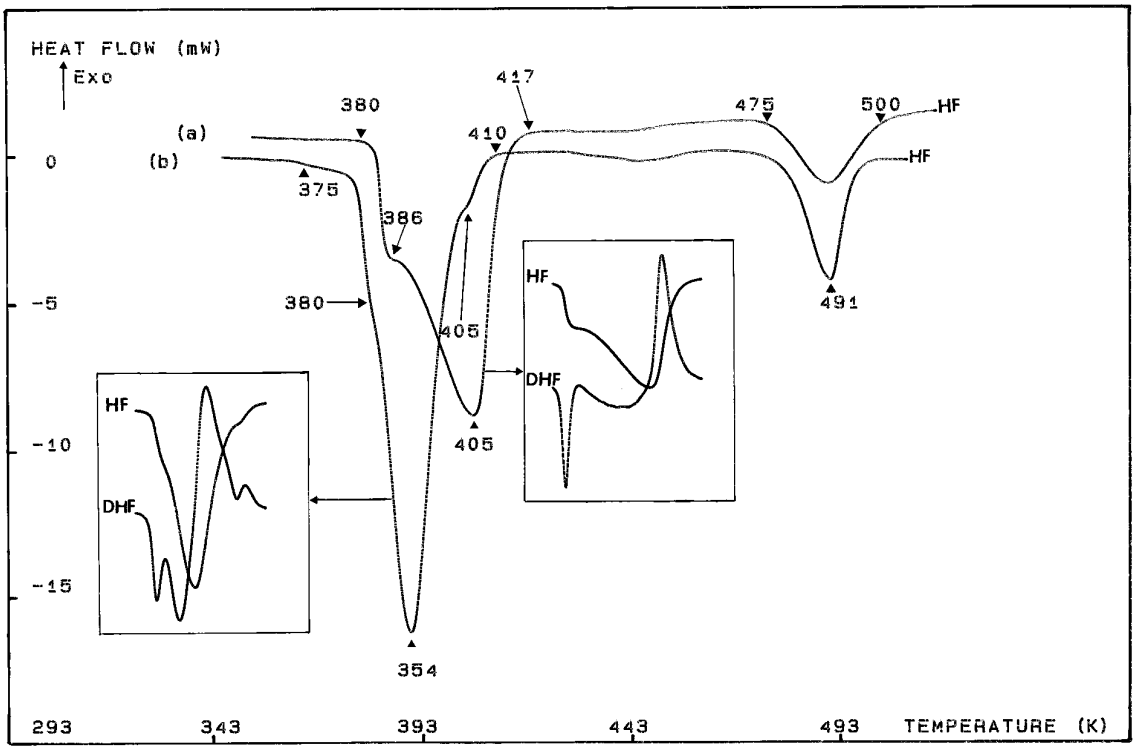

FIG. 5. DSC curves for polycrystalline samples of (a) $[C_6H_{18}N_3]_2P_6O_{18} \cdot 6H_2O$ and (b) $[C_6H_{18}N_3]_2P_6O_{18} \cdot 4H_2O$.

metry. Meanwhile some mistakes in the internal modes, calculated out, are slid, in this case, and will be corrected here. However some theoretical studies of the cyclohexasilicon group $Si_6P_6O_{18}$ (17–20) are needed for an objective assignment. The P_6O_{18} rings observed to date exhibit seven types of internal symmetry with C_i, C_2, C_s, C_{2h}, C_3, S_6, or C_1 internal symmetry. There are seven examples of a ring with a higher symmetry S_6 whereas none has the ideal local

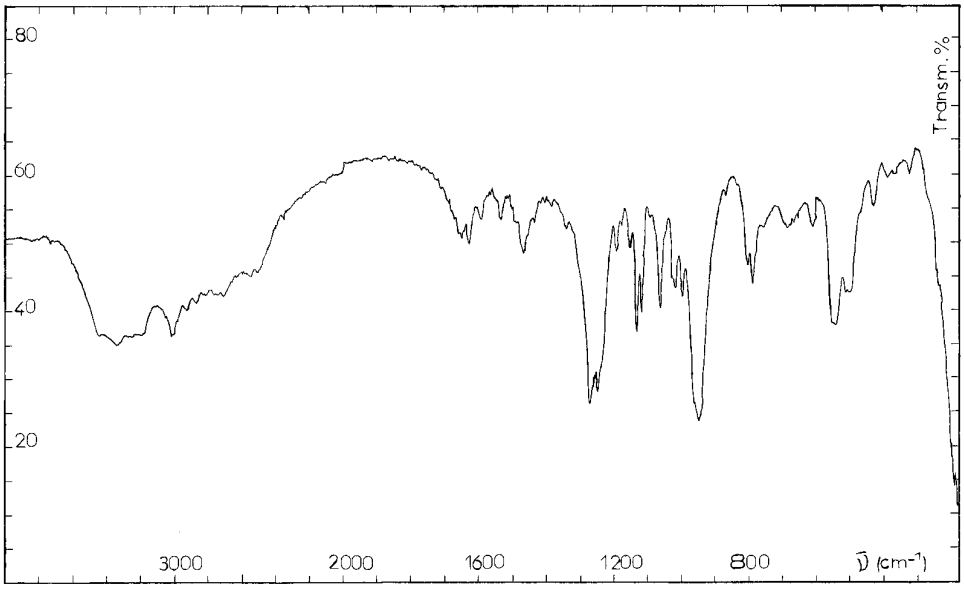

FIG. 6. IR spectrum of polycrystalline $[C_6H_{18}N_3]_2P_6O_{18} \cdot 6H_2O$.

TABLE 6
Vibrational Frequencies and Assignment in the P_6O_{18} Stretching Region

Motions	P_6O_{18}: D_{6h}			P_6O_{18}: C_i		
	IR	Ra	Modes	Modes	Ra	IR Obs. IR frequencies(cm^{-1})
$\nu_{as}OPO^-$	−	−	E_{2u}	A_u	− +	1261 vs
				A_u	− +	1247 s
	+	−	A_{2u}	A_u	− +	1192 w
	−	−	B_{2g}	A_g	+ −	
	−	+	E_{1g}	A_g	+ −	
				A_g	+ −	
ν_sOPO^-	−	−	B_{1u}	A_u	− +	1151 w
	−	+	A_{1g}	A_g	+ −	
	−	+	E_{2g}	A_g	+ −	
				A_g	+ −	
	+	−	E_{1u}	A_u	− +	1131 w
				A_u	− +	1116 s
$\nu_{as}POP$ + ν(C–C)	−	+	E_{1u}	A_u	− +	1061 s
				A_u	− +	1045 sh
	−	−	B_{2u}	A_u	− +	1018 w
	−	−	A_{2g}	A_g	+ −	
	+	−	E_{2g}	A_g	+ −	997 w
				A_g	+ −	946 vs
ν_sPOP + ν(C–C)	−	+	E_{2g}	A_g	+ −	800 w
				A_g	+ −	
	+	−	E_{1u}	A_u	− +	788 s
				A_u	− +	755 vw
	−	−	B_{1u}	A_u	− +	
	−	+	A_{1g}	A_g	+ −	684 w

Note. vs, very strong; s, strong; vw, very weak; w, weak; sh, shoulder.

symmetry D_{6h} among the presently known representatives. A ring of the type A_6B_{18} has an ideal symmetry D_{6h} and, from the 66 normal modes of vibration, classified in this point group as $\Gamma_{int.} = 4A_{1g} + 2A_{2g} + 3B_{1g} + 2B_{2g} + 4E_{1g} + 7E_{2g} + A_{1u} + 3A_{2u} + 3B_{1u} + 4B_{2u} + 6E_{1u} + 5E_{2u}$, 24 are stretching modes $\Gamma_{str.} = A_{2u} + B_{2g} + E_{1g} + E_{2u} + 2A_{1g} + 2B_{1u} + 3E_{2g} + 3E_{1u} + A_{2g} + B_{2u}$ and 42 are bending modes $\Gamma_{ben.} = 2A_{2u} + B_{2g} + 3E_{1g} + 4E_{2u} + 2A_{1g} + B_{1u} + 4E_{2g} + 3E_{1u} + A_{2g} + 3B_{2u} + 3B_{1g} + A_{1u}$. Of these, only the A_{2u} and E_{1u} modes will be infrared active in an isolated ring, and those of A_{1g}, E_{1g}, and E_{2g} in the Raman. For instance, the number of A_{1g}, B_{2g} and of B_{1u}, B_{2u} modes is inverted in analysis of P_6O_{18} ring in $[C_4H_{16}N_3]_2P_6O_{18} \cdot 2H_2O$ (2). Nevertheless crystals of the later compound belong to the C_i space group and there is one P_6O_{18} ring per unit cell, at a site of C_i symmetry. Therefore the selection rules governing P_6O_{18} in the solid are the same as they would be for the free gaseous groups. This most fortunate case allows the interpretation of the spectra of other compounds by correlation with the normal frequencies of the $P_6O_{18}^{6-}$ ring anion. Furthermore, the P_6O_{18} in the title compound has the same C_i local symmetry. The IR spectrum of $[C_6H_{19}N_3]_2P_6O_{18} \cdot 6H_2O$ is depicted in Fig. 6. The observed frequencies reported in Tables 6 and 7 are assigned according to the following features deduced from the selection rules using molecular and site symmetries and from the literature (2, 16–21): (i) Since the same atomic motions are involved in the different cyclophosphoric ring anions, the IR spectra of organic cyclohexaphosphates are divided into three regions. Frequencies in the range 4000–1340 cm^{-1} are attributed to O(N,C)–H stretching and bending modes, those ranging from 1340 to 670 cm^{-1} to asymmetric and symmetric stretching OPO^- and POP atomic groups in P_6O_{18}, and those below 670 cm^{-1} to bending, translation, and rotation of the P_6O_{18} ring. NH_3 torsion and C–C bending may occur in the latter region. (ii) The A_{2u}, B_{1u}, B_{2u}, and E_{2u} inactive modes in the D_{6h} molecular group will be active in the C_i site symmetry. Each single mode transforms into the A_u mode, whereas E_{2u} splits, like E_{1u}, into a doublet ($2A_u$). (iii) The 12 A_u (IR active) modes are distributed as a single and a doublet in each region of the following four stretching domains: 1340–1180 cm^{-1} for $\nu_{as}OPO^-$, 1180–1080 cm^{-1} for ν_sOPO^-, 1060–940 cm^{-1} for $\nu_{as}POP$, and 850–680 cm^{-1} for ν_sPOP. When the symmetry is lowered, the number of fundamentals is increased by activation of inactive modes with splitting of internal modes.

TABLE 7
Tentative Assignment of the Observed IR Frequencies Outside the Stretching Domain of the P_6O_{18} Ring Anion

$\bar{\nu}$(cm^{-1})	Attributions	$\bar{\nu}$(cm^{-1})	Attributions
3436 m	$\nu(OH_2)$ + $\nu(NH_3)$ + $\nu(NH_2)$ + $\nu(NH)$ + $\nu(CH_2)$	1490 w	$\delta(CH_2)$ + $\rho(CH_2)$ + $\omega(CH_2)$
3340 m		1470 m	
3180 w		1460 sh	
3020 m		1435 vw	
2924 vw		1410 vw	
2860 vw		1400 vw	
2700 w		1380 vw	
2740 vw	Bands of combination and harmonics	1340 w	
2700 w		1320 sh	
2540 w		611 w	$\delta(OPO^-)$ + $\delta(POP)$ + NH_3 rocking + C–C bending + NH_3 torsion
2500 w		545 s	
2350 vw		532 s	
2240 vw		514 m	
2100 vw		504 m	
1665 vw	$\delta(OH_2)$ + $\delta(NH_3)$ + $\delta(NH_2)$	470 sh	
1650 w		425 m	
1630 m		385 w	
1600 m		365 w	
1540 vw		320 m	
1530 m			

Note. s, strong; m, middle; w, weak; vw, very weak; sh, shoulder.

Thus, one should bear in mind that the total number of observed bands in the stretching domain is not definitely significant since there are two P_6O_{18} groups in the unit cell. In accordance with these considerations, the IR spectrum can be assigned as follows:

—The observed IR frequencies (single 1192 cm^{-1}, doublet 1247–1261 cm^{-1}) are assigned to the $A_u(C_i)$ modes resulting from the transformation of A_{2u} (D_{6h}) and the activation with splitting of E_{2u} (D_{6h}) modes.

—The splitting of E_{1u} (D_{6h}) and the activation of B_{1u} (D_{6h}) and B_{2u} (D_{6h}) modes give rise to doublet and single IR bands, respectively, assigned as 1151 cm^{-1} and 1131–1116 cm^{-1} for ν_sPOP, 1018 cm^{-1} and 1061–1045 cm^{-1} for ν_{as}POP, and 755 cm^{-1} and 800–788 cm^{-1} for ν_sPOP, with $\Delta\nu$ in doubled less than 17 cm^{-1}.

—Bands appearing in ν_{as}POP and ν_sPOP stretching domains at frequencies of 997, 946, and 684 cm^{-1} may be considered either ν(C–C) stretching or induced by some coupling between the two P_6O_{18} groups of the cell.

—A detailed interpretation of bands out of the P_6O_{18} stretching domain is rather difficult. Nevertheless, the comparison with spectra of other organic and inorganic compounds (22–27) leads to the frequencies reported in Table 7 with assignments of tentative character.

VI. CONCLUSION

The bis[1-(2 ammoniumethyl)-piperazinum] cyclohexaphosphate hexahydrate has been prepared in single crystal form and investigated by X-ray diffraction, thermal analyses, and vibrational spectroscopy. The geometrical characteristics of both inorganic and organic ions are examined. The main feature of this structure is the formation of anionic layers realized from $P_6O_{18}^{6-}$ that aggregates through water molecule hydrogen bonds in the (**a**, **b**) plane. These layers are connected together through a short hydrogen-bond network originating from organic cations. Thermal behavior investigated by TG-DTA and DSC analyses shows that the title compound is not very stable, since it led to a constant tetrahydrate phase when it was left standing for six months under normal conditions. The infrared study based on theoretical group analysis and on data in literature allows the interpretation of the IR spectrum.

ACKNOWLEDGMENTS

The authors express their gratitude to Dr. T. Jouini, Département de Chimie, Faculté des Sciences de Tunis, Tunisia, for the X-ray data collection.

REFERENCES

1. U. Schülke and R. Kayser, *Z. Anorg. Allg. Chem.* **531,** 167 (1985).
2. A. Gharbi, A. Jouini, and A. Durif, *J. Solid State Chem.* **114,** 42 (1995).
3. M. Charfi and A. Jouini, *Acta Crystallogr. C* to appear (1996).
4. G. M. Sheldrick, *Acta Crystallogr. A* **46,** 467 (1990).
5. G. M. Sheldrick, "SHELXL93. Program for the Refinement of Crystal Structures." University of Göttingen, Germany.
6. M. T. Averbuch-Pouchot and A. Durif, *Acta Crystallogr. C* **42,** 129 (1986).
7. A. Jouini, M. Dabbabi, and A. Durif, *J. Solid State Chem.* **60,** 6 (1985).
8. M. T. Averbuch-Pouchot, *Z. Anorg. Allg. Chem.* **570,** 138 (1989).
9. A. Durif, "Crystal Chemistry of Condensed Phosphates." Plenum, New York, 1995.
10. M. T. Averbuch-Pouchot and A. Durif, *C. R. Acad. Sci.* **308(2),** 1699 (1989).
11. M. T. Averbuch-Pouchot, *Acta Crystallogr. C* **47,** 1150 (1991).
12. O. Kennard and R. Taylor, *J. Am. Soc.* **104,** 5063 (1982).
13. G. R. Desiraju, *Acc. Chem. Res.* **24,** 290 (1991).
14. T. Steiner and W. Saenger, *J. Am. Soc.* **115,** 4540 (1993).
15. T. Steiner and W. Saenger, *Acta Crystallogr. B* **50,** 348 (1994).
16. M. Rzaigui, *J. Solid State Chem.* **89,** 340 (1990).
17. A. M. Prima, *Opt. Spectrosc.* **9,** 236 (1960) [*Opt. Spectrosc.* **9,** 452 (1960)].
18. F. Matossi, *J. Chem. Phys.* **17(8),** 679 (1949).
19. A. N. Lazarev, *Opt. Spectrosc.* **12,** 28 (1968) [*Opt. Spectrosc.* **12,** 60 (1968)].
20. A. N. Lazarev, "Vibrational Spectra and the Structure of Silicates." Sciences Press, Leningrad, Russia, 1968.
21. A. Rulmont, R. Cahay, M. Liegeois-Duyckaerts, and P. Tarte, *Eur. J. Solid State Inorg. Chem.* **28,** 207 (1991).
22. F. Scheinmann, "An Introduction to Spectroscopic Methods for the Determination of Organic Compounds," Vol. 1, Pergamon, New York, 1970.
23. N. B. Colthup, L. H. Daly, and S. E. Wilberley, "Introduction to Infrared and Raman Spectroscopy," 2nd ed. Academic Press, New York, 1975.
24. Z. Iqbal, H. Arend, and P. Washter, *J. Phys. C. Solid State Phys.* **14,** 1497 (1981).
25. S. Skaarup and W. Berg, *J. Solid State Chem.* **26,** 198 (1989).
26. D. Philip and G. Aruldhas, *J. Solid State Chem.* **83,** 198 (1981).
27. Y. Abid, M. Kamoun, A. Daoud, and F. Romain, *J. Raman Spectrosc.* **21,** 709 (1990).